

# MASS TRANSFER IN TURBULENT FLOW

R. I. LARSON\* and S. YERAZUNIS

Division of Fluids, Chemical and Thermal Processes, Rensselaer Polytechnic Institute, Troy, New York, U.S.A.

(Received 21 December 1970 and in revised form 17 February 1972)

**Abstract.** The local mass transfer coefficient in turbulent duct flow was measured using a new experimental technique. The experimental results agreed quite well with a numerical solution to the turbulent diffusion equation in channel flow. Formulation of the diffusion equation provided a continuous solution from a point near the discontinuity in mass flux to the fully developed region. The Nusselt numbers obtained numerically agreed with Spalding's asymptotic solution at  $x/D_h < 0.02$  and Hatton *et al.*'s eigenvalue solution for symmetrical heat transfer which is valid for  $x/D_h > 1$ . Current asymmetric heat transfer results in the fully developed region fell between the eigenvalue and numerical solutions.

## NOMENCLATURE

$f$ ,	friction factor ;
$D$ ,	diffusion coefficient ;
$D_h$ ,	hydraulic diameter ;
$E$ ,	eddy diffusivity of mass ;
$E'$ ,	a constant ;
$k$ ,	a constant ;
$N_{Nu}$ ,	Nusselt number ;
$N_{Pr}$ ,	(molecular) Prandtl number ;
$N_{Pr_t}$ ,	turbulent Prandtl number ;
$N_{Re}$ ,	Reynolds number based upon hydraulic diameter ;
$N_{Sc}$ ,	(molecular) Schmidt number ;
$N_{Sc_t}$ ,	turbulent Schmidt number ;
$N_{St}$ ,	Stanton number ;
$Sp$ ,	Spalding function ;
$u$ ,	longitudinal velocity ;
$u^*$ ,	friction velocity ;
$v$ ,	velocity normal to wall ;
$w$ ,	mass of diffusing species per unit mass of mixture ;
$x$ ,	distance in longitudinal direction ;
$x^+$ ,	dimensionless distance along the duct ;
$y$ ,	distance normal to wall ;
$y^+$ ,	dimensionless distance normal to wall ;

$\epsilon$ ,	eddy viscosity ;
$\epsilon_u^+$ ,	dimensionless total viscosity ;
$\epsilon_D^+$ ,	dimensionless total diffusivity of mass ;
$\nu$ ,	kinematic viscosity ;
$\zeta$ ,	dimensionless distance from the wall ;
$\rho$ ,	density ;
$\tau$ ,	shear stress.

## Subscripts

$b$ ,	bulk fluid conditions ;
$h$ ,	opposite wall conditions ;
$w$ ,	wall conditions.

## 1. INTRODUCTION

IN GAS absorption, evaporation into gas streams and partial condensation the mass transfer process may often involve the diffusion of a solute through a nontransferring gas in turbulent flow. To obtain a better understanding of the phenomena this investigation compares new asymmetric mass transfer data in turbulent flow with a theoretical analysis of the mass transfer process. The experiments measured the local mass transfer coefficient at one wall of a rectangular duct from which water was evaporated. Recent work on the heat transfer theory through turbulent boundary layers provided the basis for analyzing the experimental results.

\* Richard I. Larson is now with the General Electric Co., Schenectady, New York.

Current boundary layer heat transfer theories are distinguished from earlier efforts by the fact that the solutions are based on a partial differential equation for convective heat transfer in which the flow field is characterized by a "universal" velocity profile. These new models unlike their predecessors, the Couette flow models, include temperature variation in the flow direction. However, the assumption of uniform fluid properties and knowledge of the wall shear stress remain as part of the derivation.

Spalding [1] formulated the turbulent boundary layer heat transfer problem with the temperature field described in terms of a partial differential equation having  $x^+$  and  $u^+$  coordinates. Kestin and Persen [2], Gardner and Kestin [3], and Smith and Shah [4] obtained numerical solutions to this equation for different boundary conditions and Prandtl numbers.

Hatton and Quarmby [5] and Hatton, Quarmby and Grundy [6] investigated the heat transfer process for turbulent flow between two parallel plates. Their studies involved a partial differential equation written in terms of  $x/D_h$  and  $y^+$  coordinates. The temperature field was determined by an eigenvalue solution to the differential equation.

The mass transfer analysis described below is based on Spalding's boundary layer theory. A continuous numerical solution to the diffusion equation is obtained for all axial locations extending from a point near the discontinuity in mass flux to the fully developed region. By analogy of the heat and mass transfer processes, the numerical solution is compared with Spalding's boundary layer theory, and Hatton, Quarmby and Grundy's eigenvalue solution for developing and fully developed flow. The experimental results for asymmetric mass transfer are then examined with respect to the numerical solution of the diffusion equation.

## 2. THEORETICAL ANALYSIS

### 2.1 Diffusion equation

The concentration field in a uniform-property turbulent fluid described by the universal

velocity profile can be formulated into a partial differential equation analogous to the thermal energy equation derived by Spalding [1]. The analogous diffusion equation has the following form:

$$\rho u \frac{\partial w}{\partial x} + \rho v \frac{\partial w}{\partial y} = \frac{\partial}{\partial y} \rho (\mathcal{D} + E) \frac{\partial w}{\partial y}. \quad (1)$$

To solve this equation the wall shear stress must be known and the shear stress distribution in the fluid specified. In Spalding's analogous boundary layer formulation, the shear stress is assumed to be independent of the distance from the wall. At low mass transfer rates in channel flow with uniform fluid properties, the wall shear stress can be determined from previous work, while the shear stress distribution in the fluid is linear. The two dimensional diffusion equation reduces to the form given below by performing a von Mises transformation and by assuming the universal velocity profile,  $u^+ = f(y^+)$ , describes the flow field.

$$\frac{\partial w}{\partial x^+} = \frac{1}{u^+} \left( \frac{du^+}{dy^+} \right) \frac{\partial}{\partial u^+} \varepsilon_D^+ \left( \frac{du^+}{d\Gamma^+} \right) \frac{\partial w}{\partial u^+} \quad (2)$$

where:

$$\varepsilon_D^+ = \frac{1}{N_{Sc}} + \frac{E}{v} = \frac{1}{N_{Sc}} + \frac{\varepsilon}{v} \left( \frac{1}{N_{Sc}} \right) \quad (3a)$$

$$\varepsilon_u^+ = 1 + \frac{\varepsilon}{v} = \frac{\tau}{\tau_w} \frac{dy^+}{du^+} = \left( 1 - \frac{y^+}{y_{h/2}^+} \right) \frac{dy^+}{du^+} \quad (3b)$$

$$x^+ = \int_{x_0}^x \frac{u_*}{v} dx. \quad (3c)$$

This equation can be simplified to a parabolic form by defining a new variable,  $\xi$ .

$$\frac{\partial w}{\partial x^+} = \frac{1}{u^+ \varepsilon_D^+} \frac{\partial^2 w}{\partial \xi^2} = \frac{1}{f(\xi)} \frac{\partial^2 w}{\partial \xi^2} \quad (4)$$

and

$$\xi = \int_0^{u^+} \frac{(dy^+/du^+)}{\varepsilon_D^+} du^+. \quad (5)$$

A numerical solution was obtained for the following initial and boundary conditions.

*Initial conditions.*

$$w = 0, x^+ = 0, u^+ (\text{or } \xi) \geq 0 \quad (6)$$

*Boundary conditions.*

Asymmetric mass transfer

$$\left. \frac{\partial w}{\partial \xi} \right|_{\xi=0} = \text{constant}; x^+ > 0, u^+ (\text{or } \xi) = 0 \quad (7a)$$

$$\left. \frac{\partial w}{\partial \xi} \right|_{\xi=h} = 0, x^+ > 0, u_h^+ (\text{or } \xi) = 0. \quad (7b)$$

Symmetric mass transfer

$$\left. \frac{\partial w}{\partial \xi} \right|_{\xi=0} = \left. \frac{\partial w}{\partial \xi} \right|_{\xi=h} = \text{constant}, x^+ > 0. \quad (8)$$

### 2.2 Eddy viscosity and eddy diffusivity of mass

Spalding's expression for the velocity distribution was used to determine the eddy viscosity and eddy mass diffusivity. In channel flow the dimensionless eddy viscosity is given by:

$$\begin{aligned} \epsilon_u^+ = \frac{1}{y_{h/2}^+} & \left[ y_{h/2}^+ - u^+ - \frac{1}{E'} \left( \exp(ku^+) \right. \right. \\ & \left. \left. - 1 - ku^+ - \frac{(ku^+)^2}{2} - \frac{(ku^+)^3}{3!} \right) \right] \\ & \left[ 1 + \frac{k}{E'} \left( \exp(ku^+) - 1 - ku^+ - \frac{(ku^+)^2}{2} \right) \right] \quad (9) \end{aligned}$$

and is obtained from Spalding's single equation for the "law of the wall."

$$y^+ = u^+ + \frac{1}{E'} \left[ \exp(ku^+) - 1 - ku^+ - \frac{(ku^+)^2}{2} - \frac{(ku^+)^3}{3!} \right]. \quad (10)$$

In the central region of the channel the eddy viscosity is assumed to be constant at that value corresponding to one quarter of the distance from both walls.

To determine the eddy mass diffusivity,  $\epsilon_D$ ,

the turbulent Schmidt number is assumed to be constant throughout the flow field at a value of 0.86. Selection of this value was based upon the reviews presented by Kestin and Richardson [7] and Spalding [8].

The Reynolds number is determined by integrating the  $f(\xi)$  profile ( $f(\xi) = u^+ \epsilon_D^+$ ):

$$N_{Re} = 4 \int_0^{h/2} u^+ dy^+ = 4 \int_0^{\xi_{h/2}} f(\xi) d\xi. \quad (11)$$

### 2.3 Calculation and presentation of results

Solution of the diffusion equation is accomplished using the Crank-Nicolson implicit method, together with the "successive over-relaxation" iterative scheme to increase the rate of convergence. This numerical method is outlined by Smith [9].

The solution to the diffusion equation for internal channel flow is expressed in terms of the Spalding function, i.e.

$$Sp = \frac{N_{St}}{\sqrt{(f/8)}} = \frac{-(\partial w / \partial \xi)_{\xi=0}}{w_w - w_b} \quad (12)$$

where the bulk concentration,  $w_b$  in  $w - \xi$  coordinates is given by:

$$w_b = \frac{\int_0^{\xi_h} f w d\xi}{\int_0^{\xi_h} f d\xi} \quad (13)$$

The Spalding function and axial distance,  $x^+$ , are related to the Nusselt number and dimensional distance,  $x/D_h$ , by the following formulas:

$$N_{Nu} = Sp(f/8)^{1/2} N_{Re} N_{Sc} \quad (14)$$

$$x/D_h = x^+ / (N_{Re} \sqrt{f/8})^{1/2}. \quad (15)$$

To determine the friction factor,  $f$ , the von Kármán equation was used:

$$\frac{1}{\sqrt{(f)}} = 2.0 \log_{10} (N_{Re} \sqrt{f/8})^{1/2} - 0.8. \quad (16)$$

The wall shear stress, assumed to be known in the formulation of the diffusion equation, can be easily calculated from the above expression. Harnett, Koh and McComas [10] have previously shown that the above friction factor equation is valid in channel and duct flow over a wide range of flow conditions.

### 3. EXPERIMENTAL APPARATUS

Measurement of the local turbulent mass transfer coefficient was performed by evaporating water into a fully developed turbulent air stream flowing inside a 3 by 1 in. duct. To establish the turbulent field an entrance length of 96 hydraulic diameters separated the air stream heaters and the mass transfer test section. A schematic diagram of the equipment is shown in Fig. 1.

An electrically heated 400 mesh stainless steel wire cloth formed one of the 3 in. wide walls of the 36 in. long mass transfer test section. A 1 in. deep cavity located below the wire cloth contained the fluid to be evaporated. The wire cloth not only provided the energy for evaporation but also stabilized the gas-liquid interface through the capillary forces originating

with the surface tension of the fluid and the small size of the pores in the cloth. The axial concentration profile at the vapor-interface was determined from temperature measurements made at selected axial locations. These measurements described in more detail by Larson [11] were performed with thermocouple microprobes, positioned 10-16 mils below the screen to within an accuracy of  $\pm 0.0005$  in. The difference between the temperature as measured in the cavity and the surface temperature was shown to be less than  $0.5^\circ\text{F}$  by an analysis of the conductive heat transfer process within and below the screen apertures. The analysis was partially confirmed experimentally by measuring the temperature gradients below the screen. The concentration of vapor at the interface was determined by assuming vapor-liquid equilibrium.

The average evaporation rate (mass flux) was determined by measuring time required to empty a calibrated glass vessel. Using this average value, the axial distribution of mass flux was determined by including the effect of simultaneous heat and mass transfer to or from the air stream. The maximum variation of local

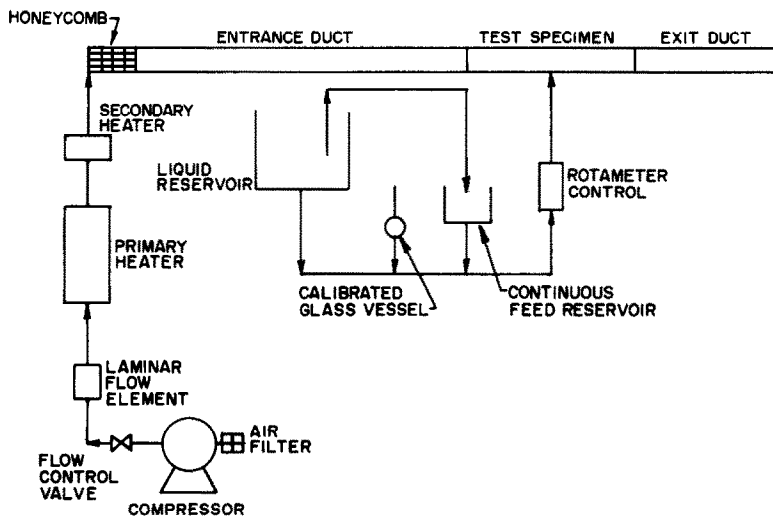


Fig. 1. Schematic diagram of experimental apparatus.

mass flux from inlet to outlet was 6 per cent. Heat transfer to or from the air stream played a small role in the evaporation process, since the electrically heated wire cloth provided 96–99 per cent of the energy for evaporation. An error analysis showed a maximum error of 9.6 per cent in measuring the local mass transfer coefficient. This analysis included the maximum error in the measurements of the evaporation rate, the interface concentration, and the density, velocity, and viscosity of the air stream. The interface concentration contributed the largest error, 6.2 per cent. This was caused by a maximum deviation in the axial temperature profile of 2°F from the average. The temperature across the width of the duct also showed a 2°F variation.

4. DISCUSSION

4.1 Comparison of the theoretical analysis with other work

Spalding [8] derived an asymptotic solution to equation 2 that was valid at small values of  $x^+$  with  $N_{Sc} = N_{Sc_i}$ . The following expression was obtained for a constant mass flux boundary condition:

$$\frac{N_{St} N_{Sc}}{(f/8)^{1/2}} = 0.651 \left( \frac{x^+}{N_{Sc}} \right)^{-1/4} \quad (17)$$

An earlier solution by Lighthill to the diffusion equation in laminar flow gives the same formula. The difference in the above expression and the numerical solution was found to be less than one per cent at values of  $x^+$  less than 10 ( $x/D_h = 0.02$  at  $N_{Re} = 7148$ ). Beyond this value of  $x^+$  the numerical results for channel flow departed from the asymptotic solution (see Fig. 2).

In the developing and fully developed region the numerical solution for symmetrical heat or mass transfer was in excellent agreement with Hatton, Quarmby and Grundy's [6] eigenvalue solution to the analogous thermal energy equation for turbulent flow between parallel plates. Hatton *et al.*'s solution is limited to values of  $x/D_h$  greater than one. Thus, the numerical solution described here for symmetrical mass transfer provides a continuous solution to the diffusion equation for all values of  $x/D_h$  and is limited only to the point at which the solution is initiated. In this case the initial  $x^+$  was 0.05.

To solve the diffusion equation numerically Spalding's continuous eddy viscosity distribution modified to include the shear distribution in the fluid was used, together with a constant value for the turbulent Schmidt number, 0.86. Hatton *et al.*'s work involved Deissler's eddy viscosity profile near the wall and Azer and Chao's [13]

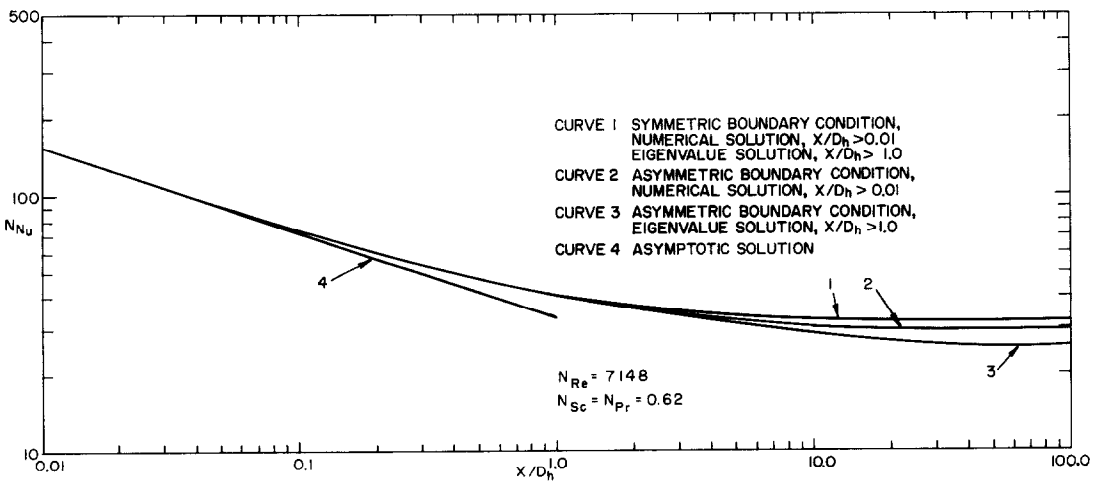


FIG. 2. Comparison of numerical solution with asymptotic and eigenvalue solutions.

expression for the turbulent Prandtl number. In an earlier paper Hatton and Quarmby's solution involved Deissler's eddy viscosity profile and a constant value of one for the turbulent Prandtl number.

The Nusselt number obtained by Hatton *et al.* for the asymmetric boundary condition was 21 per cent below the Nusselt number for symmetrical heat transfer. In our work a 9 per cent reduction was found, Fig. 2. A 10–15 per cent reduction in the Nusselt number for asymmetric boundary conditions was found in Sparrow, Lloyd and Hixon's [14] experiments on turbulent heat transfer in fully developed duct flow. These experimental data fall between the numerical results reported here and Hatton's *et al.*'s eigenvalue solution.

#### 4.2 Comparison of theoretical analysis with mass transfer measurements

Figure 3 shows the experimental data for asymmetric mass transfer in a 3 by 1 in. duct and the numerical solution of equation (2) for channel flow. Notwithstanding the secondary flow that occurs in the corners of the duct, good agreement is obtained between the experimental

data and the numerical solution at a Reynolds number of 11 200. At the high Reynolds number, 30 200, the experimental results fall below the curve by approximately 16 per cent in the fully developed flow region.

This difference can be attributed to the value of the turbulent Schmidt number, 0.86, used in solving the diffusion equation. Hatton *et al.*'s eigenvalue solutions show lower Nusselt numbers for  $Pr_t = 1$  than that determined using Azer and Chao's expression. Reductions of 18.8 and 13.5 per cent were found at Reynolds numbers of 7104 and 73 712, respectively.

Azer and Chao's equation gives values for the turbulent Prandtl number that are in good agreement with that used in our numerical solution, that is, 0.82 and 0.87 at Reynolds number of 14 500 and 43 400, respectively. If the value of the turbulent Schmidt number was increased, better agreement between the experimental data and the numerical solution would be observed at the high Reynolds number. Mass transfer data showing the Schmidt number–Reynolds number relationship to within the accuracy required by this analysis are not available and therefore, this effect is not included.

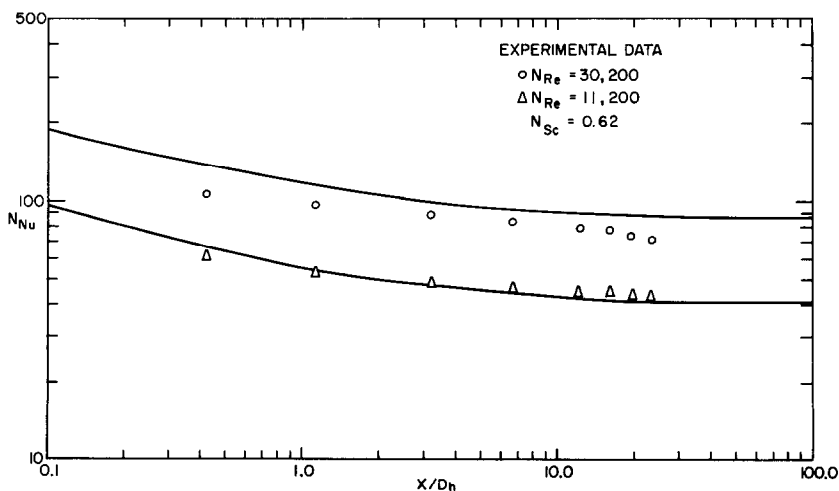


FIG. 3. Comparison of numerical solution with mass transfer results.

## 5. CONCLUSIONS

1. A new experimental technique was developed to measure the local mass transfer coefficient in turbulent duct flow. Water was evaporated into a turbulent air stream from one side of a duct using an electrically heated fine wire mesh cloth at the liquid-vapor interface. The maximum experimental error was 9.6 per cent.

2. A numerical solution to the diffusion equation describing the asymmetric mass transfer process in turbulent flow agreed quite well with the experimental results. It was also in excellent agreement with Hatton *et al.*'s eigenvalue solution for symmetrical heat transfer between parallel plates and Spalding's asymptotic solution for small values of  $x/D_h$ . The eigenvalue solution was limited to values of  $x/D_h$  greater than one. Agreement with the asymptotic solution was found at values of  $x/D_h$  less than 0.02.

3. In the fully developed region with asymmetric mass transfer, Hatton *et al.*'s solution gave a value for the Nusselt number that was 21 per cent below the symmetrical case. The numerical solution showed a 9 per cent reduction. Current heat and mass transfer experiments show a 10–15 per cent reduction.

## ACKNOWLEDGEMENT

The financial support was provided by the National Science Foundation through Grant NSF GK-350.

## REFERENCES

1. D. B. SPALDING. Heat transfer to a turbulent stream from a surface with a stepwise discontinuity of wall heat flux. *Int. Dev. Heat Transfer*, Part II, p. 439. ASME (1961).
2. J. KESTIN and L. N. PENSEN. Application of Schmidt's method to the calculation of Spalding's function and of the skin-friction coefficient in turbulent flow. *Int. J. Heat Mass Transfer* **5**, 143–152 (1962).
3. G. O. GARDNER and J. KESTIN. Calculation of the Spalding function over a range of Prandtl numbers. *Int. J. Heat Mass Transfer* **6**, 289–299 (1963).
4. A. G. SMITH and V. L. SHAH. The calculation of wall and fluid temperatures for the incompressible turbulent boundary layer with arbitrary distribution of wall heat flux. *Int. J. Heat Mass Transfer* **5**, 1179–1189 (1962).
5. A. P. HATTON and A. QUARMBY. The effect of axially varying and unsymmetrical boundary conditions on heat transfer with turbulent flow between parallel plates. *Int. J. Heat Mass Transfer* **6**, 903–915 (1963).
6. A. P. HATTON, A. QUARMBY and I. GRUNDY. Further calculations on the heat transfer with turbulent flow between parallel plates. *Int. J. Heat Mass Transfer* **7**, 817–823 (1964).
7. J. KESTIN and P. D. RICHARDSON. Heat transfer across turbulent incompressible boundary layers. *Int. J. Heat Mass Transfer* **6**, 147–189 (1963).
8. D. B. SPALDING. Contribution to the theory of heat transfer across a turbulent boundary layer. *Int. J. Heat Mass Transfer* **7**, 743–761 (1964).
9. G. D. SMITH. *Numerical Solution of Partial Differential Equations*. Oxford University Press, New York and London (1965).
10. J. P. HARNETT, J. C. Y. KOH and S. T. MCCOMAS. A comparison of predicted and measured friction factors for turbulent flow through rectangular duct. *J. Heat Transfer* **84C**, 82–88 (1962).
11. R. I. LARSON. Ph. D. dissertation. Rensselaer Polytechnic Institute, 1969.
12. M. J. LIGHTHILL. Contributions to the theory of heat transfer through laminar boundary layer. *Proc. R. Soc.* **202A**, 359 (1950).
13. N. Z. AZER and B. T. CHAO. A mechanism of turbulent heat transfer in liquid metals. *Int. J. Heat Mass Transfer* **1**, 121–138 (1960).
14. E. M. SPARROW, J. R. LLOYD and G. W. HIXON. Experiments on turbulent heat transfer in an asymmetrically heated rectangular duct. *J. Heat Transfer*. **88C**, 170–174 (1966).

## TRANSFERT MASSIQUE DANS UN ECOULEMENT TURBULENT

**Résumé**— A l'aide d'une nouvelle technique expérimentale on a mesuré le coefficient local de transfert massique lors d'un écoulement turbulent en conduite. Les résultats expérimentaux s'accordent très bien avec une solution numérique de l'équation de diffusion turbulente pour un écoulement dans un canal. La formulation de l'équation de diffusion fournit une solution continue depuis un point proche de la discontinuité dans le flux massique jusqu'à la région entièrement développée. Les nombres de Nusselt obtenus numériquement s'accordent avec la solution asymptotique de Spalding pour  $x/D_h < 0,02$  et la solution à valeur propre de Hatton et coll. pour un transfert thermique symétrique valable pour  $x/D_h > 1$ . Des résultats de transfert thermique asymétrique dans la région entièrement développée se situent entre les solutions à valeur propre et numériques.

## STOFFÜBERGANG IN TURBULENTER STRÖMUNG

**Zusammenfassung**—Der örtliche Stoffübergangskoeffizient in turbulenter Rohrströmung wurde mit Hilfe einer neuen Versuchsmethode gemessen. Die Ergebnisse stimmen sehr gut überein mit einer numerischen Lösung für die turbulente Diffusionsgleichung in Rohrströmungen. Die Diffusionsgleichung liefert eine kontinuierliche Lösung von einem Punkt in der Nähe einer Diskontinuität des Massenstroms bis in den voll entwickelten Bereich. Die berechneten Nusseltzahlen stimmen überein mit der asymptotischen Lösung von Spalding für  $x/D_h < 0,02$  und mit der Eigenwertlösung von Hatton und anderen für symmetrische Wärmeübertragung, gültig für  $x/D_h > 1$ . Die Ergebnisse für den asymmetrischen Fall im voll entwickelten Bereich fallen zwischen die Eigenwert- und die numerische Lösung.

## МАССООБМЕН В ТУРБУЛЕНТНОМ ПОТОКЕ

**Аннотация**—Локальный коэффициент массообмена в трубе измерялся по новой экспериментальной методике. Экспериментальные результаты хорошо согласуются с численными решениями с помощью уравнения турбулентной диффузии для канала. Уравнение диффузии имеет непрерывное решение от точки в окрестности разрыва массового потока до полностью развитой области. Числа Нуссельта, полученные численным методом, совпадают с асимптотическим решением Сполдинга при  $x/D_h < 0,02$  и с данными по собственным значениям на основе решений Хаттона и др. для теплообмена при симметричных условиях при  $x/D_h > 1$ . Результаты по теплообмену при несимметричных условиях в полностью развитой области лежат между собственными и численными решениями.